Dependence of the View-Angle-Tilting Technique on the Slice Orientation Angle in Correcting Susceptibility Artifacts

K-J. Jung[1,2], C-H. Moon[3], and H. Peng[1]

[1]Brain Imaging Research Center, Univ. of Pittsburgh & Carnegie Mellon Univ., Pittsburgh, PA, United States, [2]Bioengineering Department, University of Pittsburgh, Pittsburgh, PA, United States, [3]Department of Radiology, School of Medicine, University of Pittsburgh, Pittsburgh, PA, United States

Introduction: The view-angle-tilting (VAT) technique1 has been successfully applied to the correction of geometric distortion in multi-slice Fourier2 and projection-reconstruction imaging3. VAT is an attractive technique since it can correct the artifacts without post processing at the signal acquisition stage of the sequence regardless of the amplitude and polarity of susceptibility. However, it has been discovered that VAT is valid only at a specific slice orientation angle relative to the object with susceptibility.

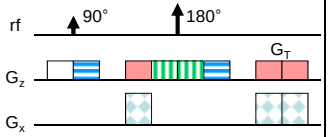

Fig. 1. A VAT pulse sequence based on the spin echo sequence.

Theory: In VAT the readout axis (*u*) is tilted by an angle θ from the conventional readout axis (*x*) toward the slice axis (*z*) when a gradient (G_T) is applied in the slice axis during the readout (Fig. **1**). The signal of a slice selective sequence for the spin density $\rho(x,z)$ with a local magnetic field inhomogeneity $h(x,z)$ can be described for the slice selection and readout as[4]

$s(t)=\int \rho(x,z)\exp[-i\phi(t)]du$, where $\phi(t)=\gamma u G_u t+\gamma(-\sin\theta/G_z+1/G_u)h(x,z)G_u t$ and $G_u=(G_x^2+G_T^2)^{1/2}$. Therefore, the inhomogeneity effect can be removed at $G_T=G_u\sin\theta$ or $G_T=G_z$. The principle of VAT is schematically explained in Fig. 2 for a cylindrical object with susceptibility. The slice at $a=-h(x,z)/G_z$ is selected at the slice selection for *z* = 0 and the selected slice is shifted along the *u* axis by $b=h(x,z)/G_u$ at the readout. The shifted slice is projected onto the *u* axis without the geometric distortion only when $b=-a\sin\theta$ or $G_T=G_z$. If this geometric condition is not satisfied, the distortion can not be corrected with VAT technique. For example, if the object with susceptibility were tilted from the slice axis, then the inhomogeneity would not be able to be corrected as illustrated in Fig. 3.

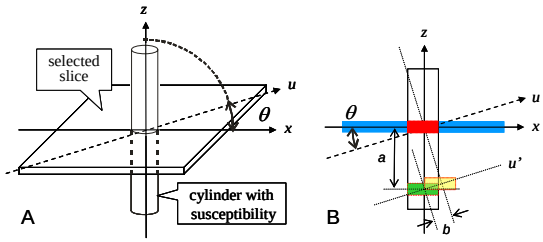

Fig. 2. Schematics of the VAT principle in the transverse slice orientation. The readout axis (*u*) axis is tilted by θ from the *x* axis to the slice axis (*z*). (A) Geometry of the imaging for a cylindrical object with susceptibility. (B) A schematic of slice selection and readout. *a* is the slice offset and *b* is the readout shift. The blue and green rectangles denote the selected slice for the homogeneous and inhomogeneous magnetic field objects, respectively. The yellow rectangle is after the readout shift by *b* and its projection onto the *u* axis is denoted by the red rectangle.

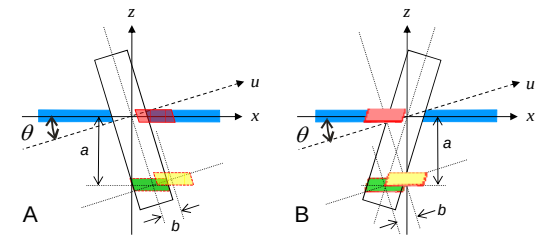

Fig. 3. Schematics of the VAT effects when the object with susceptibility is obliquely positioned from the slice axis (*z*). The color coding of the rectangles is the same as Fig. 2.

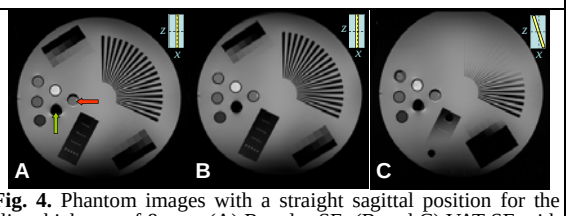

Fig. 4. Phantom images with a straight sagittal position for the slice thickness of 8 mm. (A) Regular SE. (B and C) VAT SE with θ =14° for the straight and oblique sagittal slice orientation, respectively. The insert in each slice represents the orientation of the phantom (a larger rectangle) and the slice angle (a smaller yellow rectangle). The vegetable oil and air are indicated by a red and green arrow, respectively.

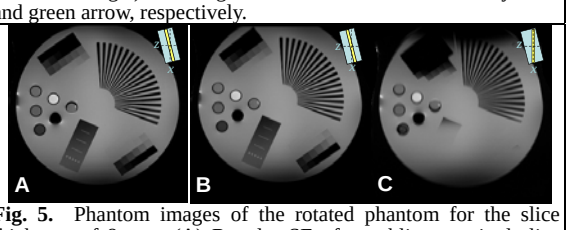

Fig. 5. Phantom images of the rotated phantom for the slice thickness of 8 mm. (A) Regular SE of an oblique sagittal slice orientation. (B and C) VAT SE for the oblique and straight sagittal slice orientation, respectively.

Methods: The computer simulation reconstructed the images of the spin echo (SE) sequence without and with the VAT gradient (G_T) by calculating the Bloch equation numerically for the cylinder with two small inserts of $\Delta\chi$ = –3.2 and 2.5 ppm. The simulation parameters were chosen to be the same as the experiments on 3T. The slice and object orientations were varied to study the effect of the slice orientation angle on the susceptibility artifacts. For the experiment, the MRI multi-purpose phantom was filled with water doped with NiSO4 and NaCl. Glass vials filled with vegetable oil and air were inserted in the phantom to induce susceptibility. The axis of the cylindrical phantom was parallel to that of the glass vials. The cylinder axis of the phantom was positioned along the x axis, i.e., in a straight sagittal orientation, so that the cylinder axis of the glass vials would be perpendicular to the main magnetic field direction (*z*). The multi-slice SE sequence was used without and with the application of the VAT gradient G_T. The readout and phase-encoding were applied along the *z* and *y* axes, respectively. The imaging parameters were FOV = 224×224 mm^2, pixel bandwidth = 224 Hz, and TR/TE = 200/16 ms. The imaging was repeated with different slice thicknesses of 8, 6, and 4 mm at which the corresponding view angles (θ) were 14.0°, 18.4°, and 26.6°, respectively. To explore the slice tilting effect further, the phantom was rotated by 14° from the *z* axis to the –*x* axis for the slice thickness of 8 mm.

Results: Dependence of VAT on the slice orientation angle was confirmed by both the computer simulation and experimentation with a phantom at 3T. When the phantom was positioned at a straight sagittal orientation (Fig. 4), the regular SE sequence produced geometric distortions at the vials containing vegetable oil and air (Fig. 4A). In VAT, the artifacts were corrected for the straight sagittal slice orientation (Fig. 4B), but they were not corrected for the oblique sagittal slice orientation (Fig. 4C). The above results were reproduced regardless of the slice thickness. When the phantom was rotated to be oblique to the z axis (Fig. 5), the susceptibility artifacts were corrected when the slice orientation was oblique in parallel with the phantom axis (Fig. 5B). However, VAT failed to correct the artifacts when the slice orientation was a straight sagittal orientation (Fig. 5C). In conclusion, VAT is a very useful technique in correcting the geometric shift due to susceptibility in slice selective imaging, but it works only when the slice orientation is in parallel with the object orientation. It should be applied carefully with an understanding of the dependence of VAT on the slice axis angle relative to the object axis with susceptibility.

References: **1**. Cho ZH, et al., *Med Phys* 1988;15(1):7-11. **2**. Butts K, et al. *J Magn Reson Imaging* 1999;9(4):586-595. **3**. Jung KJ, Cho ZH. *Magn Reson Med* 1991;19(2):349-360. **4**. Reichenbach JR, et al. *J Magn Reson Imaging* 1997;7(2):266-279.